An enthalpy based discrete thermal modelling framework for particulate systems with phase change materials

T. Zhao, Y.T. Feng

PII: S0032-5910(19)30471-1
DOI: https://doi.org/10.1016/j.powtec.2019.06.028
Reference: PTEC 14432

To appear in: *Powder Technology*

Received date: 1 April 2019
Revised date: 13 June 2019
Accepted date: 14 June 2019" role="suppressed

Please cite this article as: T. Zhao and Y.T. Feng, An enthalpy based discrete thermal modelling framework for particulate systems with phase change materials, Powder Technology, https://doi.org/10.1016/j.powtec.2019.06.028

AN ENTHALPY BASED DISCRETE THERMAL MODELLING FRAMEWORK FOR PARTICULATE SYSTEMS WITH PHASE CHANGE MATERIALS

T. Zhao, Y. T. Feng*

Zienkiewicz Centre for Computational Engineering, Swansea University, UK

Abstract

The latent thermal energy storage of phase change materials (PCM) is an attractive technique to use renewable energy. Systems with PCM capsules can be found in a wide variety of applications, but PCMs are usually approximated as a continuous phase in previous studies. The current work investigates this problem from the discontinuous point of view. The main objective is to develop an enthalpy based discrete thermal formulation that can take both heat conduction and phase change transition into consideration. The computational aspect of the formulation is fully discussed. The resulting algorithm is simple and effective. Its validity is demonstrated by solving a discrete/particle version of the one-phase Stenfan problem. In addition, the equivalent thermal properties of bulk particle materials with phase change are also derived based on a simple multi-scale modelling scheme. Numerical simulations are conducted to illustrate the effectiveness of the proposed enthalpy based discrete thermal modelling (DTEM) framework.

KEYWORDS: Phase change material; Discrete thermal element method; Effective thermal conductivity; Stefan problem

Nomenclature

α	Contact angle
β	Thermal expansion coefficient
$\mathbf{K}_{\text{eff}}$	Effective thermal conductivity, W/(mK)

* Corresponding author; e-mail: y.feng@swansea.ac.uk

$\mathbf{n}$	Outward oriented unit boundary normal
$\mathbf{x}$	Relative coordinate of the particle
ΔT	Temperature difference, °C
λ	Freezing constant
v	Poisson's ratio
v_s	Solid volume fraction
ρ	Density, kg/m^3
θ	Heating or cooling rate of the DSC measurement
ε	Thermal resistance per unit length, K/(mW)
ξ	Phase transition parameter
a	Contact radius, m
b	Pipe length, m
C_p, C, c	Specific heat capacity, J/(kgK)
C_{app}	Apprent heat capacity, J/(kgK)
E	Young's modulus, Pa
E^*	Effective Young's modulus, Pa
F_n	Normal force, N
H	Enthalpy, W
K	Contact conductance, W/K
k	Thermal conductivity, W/(mK)
L	Latent heat, W
m_{PCM}	Mass of the phase change material, kg
N	Number of particles
Q	Heat flux, W/s
q	Heat flow, W
R	Thermal resistance, K/W
r	Current radius of particles, m
r^*	Effective radius of particles, m
r_0	Initial radius of particles, m
T	Temperature, °C

V Particle volume, m^3 m 3

v Heat diffusivity, m^2/s

1 Introduction

The use of renewable energy, such as solar energy, has received much attention worldwide with the increase of energy shortage and environmental considerations. To reduce the time discrepancy between the energy production and the consumption, it is necessary to improve thermal energy storage (TES) techniques. Generally, solar heat energy can be stored in different ways including sensible heat, latent heat, or thermo-chemical reaction heat. In latent heat storage systems, the thermal energy is stored when the phase change material (PCM) undergoes a phase change, usually from solid to liquid. With the advantages of having a high density of energy storage and a narrow range of the operational temperature, the latent thermal energy storage is a particularly attractive technique [1, 2, 3, 4].

The PCM needs to be contained properly for the successful utilisation in a latent thermal energy storage system. The most common type of PCM containment is macro-encapsulation in which a significant quantity of PCM is packaged in tubes, pouches, spheres, panels or other receptacles [5]. An undesirable property of PCM is its relatively low thermal conductivity. Therefore, it is needed to increase the surface/volume ratio to improve the heat transfer rate. The packed bed TES system is developed by packing a large number of small PCM particles prepared by micro-encapsulation techniques with the heat transfer fluid [6]. This packed bed TES system can be found in a variety of applications, such as heating and cooling systems in buildings [1], solar thermal energy storage [2], solar cooling [3] and compressed air energy storage [4].

Since its wide applications, understanding the nature of a packed bed TES system has long been of a keen research interest. The main research methods used in previous investigations include the experiment [7, 8] and numerical simulation. Considering technological and economical barriers of the experimental work, numerous contributions have been made in the field of computational modelling to study the performance of the TES system. These numerical models can mainly be divided into two groups: single-phase model and separate-phase model. In the single-phase model [9], the packed bed is regarded as a quasi-homogeneous medium; while in the separate-phase model [10], both solid and fluid phases are considered separately with two energy conservation equations and are coupled by a heat exchange term.

An extensive comprehensive review of different numerical models for PCM packed bed systems can be found in the review article [11]. The fixed grid method [12] and the adaptive mesh method [13] are adopted to solve the boundary value problems for partial differential equations where the phase boundary can evolve with time. The solutions of the differential equations are realised by finite-difference or finite element approximations [14]. It can be realised that the solid material (granular phase changing composites obtained by micro or macro-encapsulating PCMs) of the packed bed TES system is approximated as a continuous phase in the previous studies while it is actually the discontinuous particulate system. Therefore, it is necessary to investigate this problem from the discontinuous point of view.

Since it was originated, the discrete element method (DEM) [15] has emerged as a reliable and effective numerical technique to model scientific and engineering problems involving particulate materials. Despite its extensive utilisations in the field of mechanical properties of dynamic particulate systems, DEM has also been used to simulate heat transfer in granular assemblies. Hunt [16] first introduced DEM to solve heat transfer problems of granular material flows and determined the effective thermal conductivity and self-diffusivity. Vargas et al.[17] developed the thermal particle dynamics (TPD) method based on DEM to study heat conduction in granular materials and stress effects on the conductivity of particulate beds [18]. Chaudhuri et al. [19] simulated heat transfer in granular flows in rotating vessels, in which granular flows and heat transport properties are taken simultaneously into account to understand their effects on dryer and calcination performance.

A simple particle-particle heat transfer model is used in the above researches to account for the thermal effects and may inevitably suffer from a poor solution accuracy. Feng et al.[20] proposed the discrete thermal element method (DTEM) for accurate and effective modelling of heat conduction between individual particles in particulate systems in 2D cases. This method was extended to a simplified version, termed the pipe-network model [21], which significantly simplifies the solution procedure of the original DTEM. These studies and others have demonstrated the capability of the DEM as a powerful tool for investigating heat transfer problems in particulate systems [22, 23] and for determining the corresponding effective thermal conductivity [24, 25, 26]. However, little effort has been made to investigate particulate systems with phase change materials.

The main objective of this paper is thus to develop an enthalpy based discrete thermal

formulation that can take both thermal conductivity and phase change into consideration in particle systems. The equivalent thermal properties of bulk particle materials with phase change will also be derived based on a simple multi-scale modelling scheme.

This paper is organised as follows. In Section 2, a brief description of the PCM together with its thermal material characterisation and mathematical modelling is provided. The enthalpy based DTEM framework is developed in Section 3. The computational aspect of the formulations for both heat conduction modelling and phase change modelling are fully discussed and described. In Section 4, the way to determine the effective thermal properties are addressed in detail. The validity of the DTEM method is demonstrated in Section 5 by solving a particle version of the classic one-phase Stenfan melting problem [27]. Section 6 is devoted to conduct numerical simulations which illustrate the effectiveness of the proposed method to model the particulate system of PCM capsules. The conclusion is drawn in Section 7.

2 Phase change material

Thermal energy storage is an important technology to balance the supply and demand of energy. It has been widely used in applications such as building, concentrated solar plants and thermal management of batteries [28], to name a few. A TES system can be a sensible, latent or chemical heat storage as shown in Figure 1(a). The sensible heat storage applies a temperature gradient to the material to store or release heat. The disadvantage of the sensible heat storage is the low storage capacity which leads to a huge volume of the system. The latent heat storage can provide a high storage density with a small temperature difference between storing and releasing heat. The materials used for the latent heat storage are called phase change materials and are characterised by storing large amount of thermal energy while changing from one phase to other (usually solid-liquid states) at a narrow temperature range which has been regarded as a constant temperature in some research, and presenting high heat of phase change (latent heat) [29].

The enthalpy variation with temperature of both sensible and latent materials are shown in Figure 1(b). The enthalpy-temperature relation of real materials in nature for all solid, liquid or phase change mixtures is non-linear as shown in the black line, but it is often simplified as a (piecewise) linear relation (blue line) for convenience in engineering applications. PCMs can be classified as organic and inorganic, of which the organic material paraffin is the most popular commercial PCM due to its long-term stability, suitable phase change temperature and acceptable

price.

Figure 1: Energy storage materials

2.1 Encapsulation of PCM

Main drawbacks of PCMs include low thermal conductivity, leakage, subcooling and flammability. Appropriate methods need to be developed to ensure the successful utilisation of PCMs. Containment methods can be classified as the bulk storage in tank heat exchangers, the macro or micro encapsulation. In the encapsulation process, individual particles or droplets of solids or liquid PCMs (the core) are surrounded or coated with a film of polymeric materials (the shell). This method has the advantages of providing a large heat transfer area and reducing the reactivity of the materials with the outside environment. The characteristic diameter of such granular phase change composites ranges from a few millimeters to a few centimeters. Granular phase change materials (GPCM) offer the advantage of maintaining their macroscopic solid form during phase change which is the solid component of the latent heat thermal energy storage system (LHTES) [30].

2.2 Material characterisation

The phase change of most PCMs occurs in a temperature range rather than at a constant temperature. From heat flow results of differential scanning calorimeter (DSC) measurements, the apparent heat capacity of granular PCMs is acquired as [12]

$$C_{\text{app}}(T) = \frac{q(T)}{m_{\text{PCM}}\theta} + C_p \tag{1}$$

where m_{PCM} is the mass of the PCM used in the DSC, θ is the heating or cooling rate of the DSC measurement and C_p is the specific heat of the solid or liquid PCM. Packed-bed column experiments during charging and discharging modes are usually carried out to analyse the granular phase change material [5].

2.3 Mathematical models

The complex transient nature of granular PCM systems and the high cost of the set-up for an

experimental testing makes it necessary to use numerical models to investigate PCM systems. Existing numerical models developed can mainly be divided into two groups: single or two phase model [31].

In the single phase model, the solid phase (PCM spheres) and the fluid phase are considered as one phase. Ismail and Stuginsky [32] demonstrated that this model is useful in analysing fixed beds of both high thermal conductivity and thermal capacity in comparison to the working fluid. In the two phase model, solid and fluid phases are considered separately, and the model can be classified into three (sub-)categories: the concentric dispersion model [3], the continuous solid phase model [33], and the Schumann model [10].

All the four models mentioned above assume the solid phase as a porous material, not as a medium comprised of individual particles. Thus, the accuracy of these models depends on the effective thermal conductivity of the porous material and the total heat transfer coefficient between the fluid and the solid, both of the parameters are usually determined from empirical correlations.

3 The enthalpy based DTEM framework

Considering the limitations of the continuous based models and the discontinuous nature of granular PCMs, it will be a new direction to simulate the particulate system with PCMs from the discontinuous point of view. Therefore, an enthalpy based discrete thermal modelling framework is developed in the current work. It should be noted that only the solid component (PCM spheres) is considered as the main object of this work is to propose a novel method to treat the heat conduction and phase change transition in the particulate system with PCMs rather than model a specific packed-bed column experiment.

3.1 Heat conduction modelling

Different mechanisms exist in heat transfer of particulate systems, including thermal conduction through the solid; thermal conduction through the contact area between two particles; thermal conduction to the interstitial fluid; heat transfer by fluid convection; and radiant heat transfer between the surfaces of particles [34]. According to Batchelor and O'Brien [35], when the interstitial medium is stagnant with a smaller thermal conductivity compared to that of the particles, thermal conduction through the contact area plays the dominate role in heat transfer process. Thus, the current work of heat transfer in particulate systems with phase change material

is focused on contact conductance between particles.

3.1.1 Thermal DEM

To simulate the heat transfer process in a particle system, temperature is introduced into the DEM as an additional degree of freedom. For the particulate system with a large number of particles, it is extremely time consuming to determine the temperature distribution of each particle. Thus, each particle has been assumed as iso-thermal in DEM simulations. Heat flow occurs via conduction in the active contact area that connects two particles (i and j) whose (average) temperatures are T_i and T_j respectively. The Fourier's law of heat conduction denotes the amount of heat transported across their mutual (contact) boundary per unit time as

$$Q_{ij} = K_{ij}(T_j - T_i) \tag{2}$$

where K_{ij}, termed the contact conductance, is the amount of heat transported per unit temperature difference per unit time. The evolution of the temperature of particle i is given as

$$\frac{dT_i}{dt} = \frac{Q_i}{C_i} \tag{3}$$

where Q_i is the total amount of heat transported to particle i from its neighbor particles calculated from Equation(2) as

$$Q_i = \sum_{j=1}^{N} Q_{ij} \tag{4}$$

in which N is the number of particles in contact with particle i; C_i is the total heat capacity of particle i which is defined as

$$C_i = \rho_i c_i V_i \tag{5}$$

where ρ_i, c_i and V_i are the density, specific heat capacity and volume of particle i respectively.

Equation (3) can be discretised by expressing the time derivative using, for instance, the forward finite difference to update the particle temperature as

$$T_{i\langle t+\Delta t\rangle} = T_{i\langle t\rangle} + \frac{Q_i}{C_i}\Delta t \tag{6}$$

There are two criteria that need to be satisfied in this thermal DEM method: (1) The temperature of

particle i keeps the same value at different contact points with all the neighbor particles. This requires that the resistance to heat transfer inside the particle is significantly smaller than the resistance between the contacting particles, which is generally true because the contact area is often far smaller than the size of particles; (2) The stability criterion of the explicit time integration scheme requires that the temperature change of each particle sufficiently slow so that thermal disturbances do not propagate further than its immediate neighbors during one time-step. This can be satisfied by choosing a sufficiently small time-step.

Another aspect considered in modelling of thermal conduction is the thermal expansion and contraction of the particle size. Similar to the previous treatment [36, 37, 38], the radius expansion/contraction is considered as

$$r = r_0(1+\beta\Delta T) \tag{7}$$

where r_0 is the initial radius of particles at the reference temperature T_0, r is the current radius, $\Delta T = T - T_0$ is the temperature change, and β is the thermal expansion coefficient (assuming constant in the current work).

When the thermal expansion of particles is taken into account, granular materials would exhibit the settling behavior under thermal excitations which needs to be simulated by considering kinematic of particles in conjunction with the thermal modelling. This has two consequences. One is the increase of the packing density and the other is the particle rearrangement. The packing density has a major influence on thermal properties of granular phase change materials as can be seen in Section 6.2, while the effect of particle rearrangement on thermal properties is less clear for randomly packed particle configurations.

Nevertheless, the effect of particle size change may not be significant in the thermal modelling of phase change materials as the narrow range of the operational temperature during the charging and discharging processes and the randomness of particle arrangement under thermal excitations. Thus most of the thermal simulations conducted in the current work, unless those mentioned specifically, do not consider the size expansion to reduce the computation time because the required time-step in the thermal DEM simulation is often orders of magnitude larger than the corresponding time-step in the mechanical DEM [24]. The thermal induced size change effect will be discussed in detail in Subsection 6.4.

3.1.2 Thermal contact model

To accomplish the above thermal DEM simulation, the contact conductance K_{ij} in Equation (2) needs to be determined properly. Contact conductance refers to the heat transmit ability of two touching materials. Most work related to this topic can be found in fields of microelectronics, aircraft industry, nuclear industry and nano-technologies [39]. The thermal contact model in thermal DEM modelling borrows some mature results from the early work of contact conductance [40, 41]. The approximate analytical solution of the contact conductance between two smooth, elastic spheres is often adopted to consider the heat transfer process in thermal DEM as

$$K_{ij} = 2k\left[\frac{3F_n r^*}{4E^*}\right]^{1/3} = 2ka \tag{8}$$

where k is the thermal conductivity, F_n is the normal force acting between the particles, a is the contact radius, $r^* = r_i * r_j / (r_i + r_j)$ is the effective particle radius, and E^* is the effective Young's modulus for the two particles

$$\frac{1}{E^*} = \frac{1-\nu_i^2}{E_i} + \frac{1-\nu_j^2}{E_j} \tag{9}$$

in which ν_i and ν_j are the Poisson's ratios of the two particles.

Despite the above relation (8) that is often used in most of thermal DEM simulations [17, 18, 24, 42], a thermal pipe contact model is developed in Particle Flow Code [43] in which heat flows between particles through a one-dimensional pipe where the contact conductance is defined as

$$K_{ij} = \frac{1}{\varepsilon b} \tag{10}$$

in which ε is the thermal resistance per unit length, and b is the pipe length.

The determination of the contact conductance in the above models is mainly done in an *ad hoc* manner rather than based on a rigorous theoretical foundation. Feng et al. [20, 21] proposed a 2D pipe-network model for the modelling of heat conduction in particulate systems which provides a more rational and accurate model to represent heat conduction.

In this 2D pipe-network model, one particle can be conceptually represented by a simple star-shaped pipe network model in which the centre is connected to each contact zone as shown in Figure 2.

Figure 2: Discrete thermal element and pipe-network model for disc [20, 21]

For each individual pipe j of the i th particle, the corresponding thermal resistance $R_{i,j}$ is given by

$$R_{i,j} = \frac{1}{\pi k_i}\left(-\ln \alpha_{i,j} + \frac{3}{2} + \frac{\alpha_{i,j}^2}{36} + \frac{\alpha_{i,j}^4}{2700} + \frac{\alpha_{i,j}^6}{79380} \right) \tag{11}$$

where $\alpha_{i,j}$ is the contact angle of the contact region defined as the ratio of the contact length and the particle radius. Then, the thermal contact conductance K_{ij} between the i th and j th particles is formulated as

$$K_{ij} = \frac{1}{R_{i,j} + R_{j,i}} \tag{12}$$

A similar approach can also be developed to define the thermal contact conductance for contacting spheres.

3.2 Phase change modelling

Phase change materials are viewed as latent heat storage units as a large amount of energy is absorbed or released when materials changes from solid to liquid and vice versa. In the DTEM method, the phase change transition is taken into account by using the enthalpy concept. The change in enthalpy equals to the heat absorbed or released for the enclosed system at a constant pressure. The quantity of thermal energy possibly stored depends on the enthalpy variation in the working temperature range.

In the current DTEM framework, a PCM sphere is regarded as a phase change material as shown in Figure 1, and the phase change process occurs at the temperature T_s and ends at the temperature T_l as shown in Figure 1(b), and the enthalpy variation is equal to the latent heat L. The enthalpy of each sphere is H_i and can be obtained by

$$H_{i\langle t+\Delta t\rangle} = H_{i\langle t\rangle} + Q_i \Delta t \tag{13}$$

For the phase change transition from solid to liquid, the onset enthalpy is $H_s = C_i T_s$ and the end enthalpy is $H_l = H_s + L$ as shown in Figure 1(b).

The specific capacity c_i and thermal conductivity k_i of each particle need to be modified

according to the enthalpy H_i of that particle as follows

$$c_i = \begin{cases} C_s, & H_i \le H_s \\ C_s + \dfrac{H_i - H_s}{H_l - H_s}(C_l - C_s), & H_s < H_i < H_l \\ C_l, & H_i \ge H_l \end{cases} \tag{14}$$

and

$$k_i = \begin{cases} k_s, & H_i \le H_s \\ k_s + \dfrac{H_i - H_s}{H_l - H_s}(k_l - k_s), & H_s < H_i < H_l \\ k_l, & H_i \ge H_l \end{cases} \tag{15}$$

To track the phase change evolution of a particulate system, the phase change time T_{ic} of each particle is recorded. A phase transition is assumed to occur at the time when a particle has stored or released a certain amount of the latent heat, or the phase transition latent heat $H_{pt}(\xi)$ determined by a given parameter $\xi \in [0,1]$ as

$$H_{pt}(\xi) = (1-\xi)H_s + \xi H_l \tag{16}$$

With the phase change time of each particle is known, the position evolution of the phase change front in a particulate system can be obtained in DTEM modelling.

4 Effective thermal properties

In design of a LHTES, it is necessary to properly determine thermo-physical properties including the effective thermal conductivity and other thermal properties of the system. For the particulate system of phase change material, it is not easy to characterise granular phase change composites due to the nature of the material and the heterogeneity of the sample. Small and non-uniform diameters of spherical capsules also complicate the evolution of latent heat in a heat storage system. The current DTEM method makes it possible to numerically obtain the effective thermal properties of a granular PCM system by applying a homogenisation based technique.

4.1 Effective thermal conductivity

To predict the effective thermal conductivity (ETC), $\mathbf{K}_{\text{eff}}$, of granular materials is an important subject for many scientific and industrial applications involving particulate systems. Various

experimental tests and analytical models have been proposed to measure or analyse the ETC of granular materials [44, 45, 46]. Compared to these methods, numerical simulations can be employed to obtain heat transfer of granular materials, which makes the numerical simulation using DTEM a powerful means to predict the ETC.

In theory, the ETC of granular assemblies can be determined by solving the equation of Fourier's law of heat conduction. Therefore, the heat flux $\mathbf{q}''$ and temperature gradient ∇T need to be obtained from DTEM simulations. A simple way is to obtain them from a boundary value problem where the granular sample is considered as a continuum phase. A more accurate method is to obtain the average heat flux $\langle \mathbf{q}'' \rangle$ and temperature gradient $\langle \nabla T \rangle$ of a granular assembly [24], which is analogous to compute the average stress and strain of a particulate system by using the multi-scale method [47, 48, 49]. In granular materials, the micro scale is taken to be a scale where individual particle responses are measurable, while the macro scale is where the whole assembly is considered as a continuum phase. The following description of using the average heat flux and temperature gradient to predict the ETC of a particle assembly is mainly adopted from [24].

4.1.1 Average temperature gradient

Consider the steady state heat transfer of a granular system, Ω, where the approximate temperature $\tilde{T}^i$ of each particle is expressed as

$$\tilde{T}^i = \nabla T \cdot \mathbf{x}^i \tag{17}$$

in which $\mathbf{x}^i$ is the relative coordinate of the particle, and ∇T is the temperature gradient at the macroscale level where the granular assembly is considered as a continuum phase.

Because of the fluctuation of the particle temperature distribution in the particulate system, the real temperature $\hat{T}^i$ is not exactly match the approximate temperature $\tilde{T}^i$, so

$$\hat{T}^i - \nabla T \cdot \mathbf{x}^i \neq 0 \tag{18}$$

To find the specific $\langle \nabla T \rangle$, the square sum of the deviations in Equation (18) should be minimised. Thus by employing the least-squares approach, $\langle \nabla T \rangle$ can be obtained as a solution of the following linear equations

$$\sum_{i \in \Omega} \mathbf{x}^i (\hat{T}^i - \langle \nabla T \rangle \cdot \mathbf{x}^i) = 0 \tag{19}$$

4.1.2 Average heat flux

In the state of heat equilibrium without heat sources, the temperature of each particle remains constant so the total heat exchange through the boundary of the granular assembly, $\partial\Omega$, is zero:

$$\int_{\partial\Omega}\mathbf{q}''\cdot\mathbf{n}dA=\sum_{i\in\partial\Omega}q^{ib}=0 \tag{20}$$

where $\mathbf{q}''$ is the heat flux flowing through the boundaries, $\mathbf{n}$ is the outward oriented unit boundary normal and $\int_{\partial\Omega}$ is the integration on the boundary of the particulate system, q^{ib} is the total heat flowing through the boundary contacting with particle i.

The average heat flux $\langle\mathbf{q}''\rangle$ of the particulate system is given by

$$\langle\mathbf{q}''\rangle=\frac{1}{V}\int_{\Omega}\mathbf{q}''dV=\frac{1}{V}\sum_{i\in\partial\Omega}q^{ib}\mathbf{x}^{ib} \tag{21}$$

where $V=|\Omega|$ is the volume of the particulate system and $\mathbf{x}^{ib}$ denotes the coordinates of the contact point between particle i and the boundary. Hence, the average heat flux of the particulate system can be computed from the simulation.

4.1.3 Effective thermal conductivity

By applying Fourier's law of heat conduction, the effective thermal conductivity $\mathbf{K}_{\text{eff}}$ should satisfy

$$\mathbf{K}_{\text{eff}}\langle\nabla T\rangle=-\langle\mathbf{q}''\rangle \tag{22}$$

$\mathbf{K}_{\text{eff}}$, as a tensor, is required to be symmetric and positive definite which are automatically satisfied by enforcing the symmetry of $\mathbf{K}_{\text{eff}}$ [50]. Then $\mathbf{K}_{\text{eff}}$ is obtained from solving the following overdetermined linear system of equations

$$\begin{bmatrix} {}^1T_{,1} & {}^1T_{,2} & {}^1T_{,3} & & & & & & \\ & & & {}^1T_{,1} & {}^1T_{,2} & {}^1T_{,3} & & & \\ & & & & & & {}^1T_{,1} & {}^1T_{,2} & {}^1T_{,3} \\ {}^2T_{,1} & {}^2T_{,2} & {}^2T_{,3} & & & & & & \\ & & & {}^2T_{,1} & {}^2T_{,2} & {}^2T_{,3} & & & \\ & & & & & & {}^2T_{,1} & {}^2T_{,2} & {}^2T_{,3} \\ {}^3T_{,1} & {}^3T_{,2} & {}^3T_{,3} & & & & & & \\ & & & {}^3T_{,1} & {}^3T_{,2} & {}^3T_{,3} & & & \\ & & & & & & {}^3T_{,1} & {}^3T_{,2} & {}^3T_{,3} \\ & 1 & & -1 & & & & & \\ & & 1 & & & & -1 & & \\ & & & & & 1 & & -1 & \end{bmatrix} \begin{Bmatrix} k_{11}^{eq} \\ k_{12}^{eq} \\ k_{13}^{eq} \\ k_{21}^{eq} \\ k_{22}^{eq} \\ k_{23}^{eq} \\ k_{31}^{eq} \\ k_{32}^{eq} \\ k_{33}^{eq} \end{Bmatrix} = - \begin{Bmatrix} {}^1\langle q'' \rangle_1 \\ {}^1\langle q'' \rangle_2 \\ {}^1\langle q'' \rangle_3 \\ {}^2\langle q'' \rangle_1 \\ {}^2\langle q'' \rangle_2 \\ {}^2\langle q'' \rangle_3 \\ {}^3\langle q'' \rangle_1 \\ {}^3\langle q'' \rangle_2 \\ {}^3\langle q'' \rangle_3 \\ 0 \\ 0 \\ 0 \end{Bmatrix} \tag{23}$$

where all blank coefficients of the matrix are 0 and the superscripts 1, 2 and 3 represent the boundary problems in the three directions of the Cartesian coordinate system. This equation is solved as a linear least-squares problem.

4.2 Effective latent heat

The effective latent heat L_{eff} of the particulate system of PCMs is an important property which indicates its heat storage capacity. For a granular system, the effective latent heat L_{eff} can be simply obtained as

$$L_{\text{eff}} = L\nu_s \tag{24}$$

where L is the latent heat of the granular particles, and ν_s is the solid volume fraction, or packing density, of the particulate system.

5 Validation

As our current work is to treat granular PCMs from the discontinuous point of view, its validity will be demonstrated by applying it to solve a discrete/particle version of the classical phase change problem – the Stefan problem, where a particulate system with PCMs will be treated as a one-dimension continuous medium. The interface evolution of the particulate system should be analogous to its continuum counterpart. For the continuum phase, the phase transition is described as a boundary value problem of partial differential equations (PDE), where the phase boundary

moves with time.

In the following subsections, the moving boundary Stefan problem is introduced first. The latent heat is an important parameter which affects the movement of the phase boundary (solid-liquid interface) of the system. The validity of the DTEM method will be demonstrated by comparing the actual effective latent heat L_{eff} of the particulate system with the fitted one $L_{\text{eff-fit}}$ derived from the numerical results.

Note that no thermal expansion/contraction is considered in this section. The thermal induced particle size change effect will be discussed in Section 6.4.

5.1 The Stefan problem

This classical moving boundary problem dates back to the study of the melting of glaciers by the Slovenian physicist Jozef Stefan in 1889 [27]. It aims to describe the temperature distribution in a homogeneous medium undergoing a phase change. The physical constraints of this problem are the conservation of energy and the local velocity of the interface depends on the heat flux discontinuity at the interface. From a mathematical point of view, the phases are regions in which the solutions of the underlying PDE are continuous. The moving boundary are infinitesimally thin and the PDE are not valid at phase change interfaces. Therefore, an additional Stefan Condition is needed to obtain closure. The analytical solutions for this problem is available for one-dimensional cases of an infinite region with simple initial and boundary conditions.

5.1.1 Formulations

For a semi-infinite region, the initial temperature is T_0. At time $t>0$, the temperature of the boundary at $x=0$ is suddenly kept at T_w. The governing equations for the temperature distribution $T(x,t)$ in the region are formulated as follows

$$\begin{cases} C_l \dfrac{\partial T}{\partial t} = \dfrac{\partial}{\partial x}[k_l \dfrac{\partial T}{\partial x}] & 0 < x < s(t), t > 0 \\ T_l(0,t) = T_w & t > 0 \end{cases} \tag{25}$$

$$\begin{cases} C_s \dfrac{\partial T}{\partial t} = \dfrac{\partial}{\partial x}[k_s \dfrac{\partial T}{\partial x}] & s(t) < x < +\infty, t > 0 \\ T_s(+\infty,t) = T_0 & t > 0 \end{cases} \tag{26}$$

subject to the initial condition

$$T(x,0) = T_0 \tag{27}$$

where $s(t)$ is the interface position, and the subscripts s and l indicate the solid and liquid phases.

The moving rate of the interfaces is controlled by the latent heat lost or absorbed at the boundary. The following equation, known as the Stefan Condition, describes this process.

$$k_l \frac{\partial T_l}{\partial x} - k_s \frac{\partial T_s}{\partial x} = -\Lambda \frac{ds}{dt} \quad \text{at} \quad x = s(t) \tag{28}$$

where $\Lambda = \rho L$ is the heat of phase change per unit volume (note that L is the latent heat coefficient) and ds/dt is the velocity of this interface.

Moreover, the temperature verifies:

$$T_l = T_s = T_m \quad \text{at} \quad x = s(t) \tag{29}$$

where T_m is the melting temperature.

This problem can be formulated in non-dimensional variables for a finite sheet $0 \le x \le l$ (l is a standard length) by assuming constant thermal values and using a simple scaling [51]. The non-dimensional form makes it convenient to obtain the analytical solution and save computational costs of the numerical solutions.

5.1.2 Analytical solution

The exact solution of the one-dimensional Stefan problem, available in the literature [52], can be derived by using the similarity variable to transform the governing equation from partial derivatives to an ordinary differential equation. The solution of the temperature distribution is

$$T(x,t) = T_0 - \frac{T_0}{erf(\lambda)} erf\left(\frac{x}{2\sqrt{t}}\right) \tag{30}$$

where λ is the freezing constant given by the root of the following transcendental equation

$$\lambda e^{\lambda^2} erf(\lambda) = Ste / \sqrt{\pi} \tag{31}$$

in which erf is the error function and Ste is the Stefan number defined as

$$Ste = \frac{C\Delta T}{L} \tag{32}$$

where C is the specific heat of solid phase in the freezing process, but is the specific heat of the liquid phase in the melting process; ΔT is the temperature difference between the two phases.

The moving front position is expressed as

$$s(t) = 2\lambda\sqrt{vt} \tag{33}$$

where $v = k_s / C_s\rho$ is the heat diffusivity.

5.2 Effective latent heat of a particle system based on DTEM

As mentioned in Section 3.2, the phase change time of each particle can be recorded during the simulation. The time history of the phase change times and positions of all the particles in the system will depict how the melting interface of the system evolves with time. If the particulate system is regarded as an equivalent continuum, it should have a similar relation as described by Equation (33). The phase change time - position points of the particles can be curve fitted by this relation, and then the resulting freezing constant λ can be used to derive the effective latent heat based on both Equation (31) and Equation (32). Thus, the fitted effective latent heat $L_{\text{eff-fit}}$ is derived based on the simulation results as

$$L_{\text{eff-fit}} = \frac{C\Delta T}{\lambda e^{\lambda^2} erf(\lambda)\sqrt{\pi}} \tag{34}$$

If the proposed enthalpy based DTEM method for simulations of problems with PCMs is valid, the $L_{\text{eff-fit}}$ obtained by Equation (34) should be close to L_{eff} calculated by Equation (24).

Numerical simulations using the enthalpy based DTEM method are conducted to derive the fitted effective latent heat $L_{\text{eff-fit}}$ of a particulate system with granular PCMs. Three cuboid shaped boxes with 1m in both length and width and 5m in height filled with PCM capsules have been randomly generated with some initial contacts between neighbouring particles. These samples have different packing densities $\nu_s = 0.6, 0.65$ and 0.7 respectively. The diameters of the capsules have a uniform distribution between 0.05m to 0.06m.

The top and bottom of each box have a constant temperature of 100 ° C and 60 ° C respectively. Heat is conducted between the top and bottom of the box with the contacting particles in the sample. The side surfaces of the boxes are adiabatic or insulated. The initial temperature of all the PCM capsules is 60 ° C. It is assumed that the particles are ideal phase change materials and the melting process occurs at a temperature point $T_m = 60°\,\text{C}$ rather than a temperature range. The phase transition latent heat H_{pt} is set by choosing the parameter $\xi = 0.5$. A particle is assumed

melted when the enthalpy of the particle $H \geq H_{pt}$. The thermal properties of the PCM capsules are set as $C_p = 430\text{J}\cdot\text{kg}^{-1}\cdot\text{K}^{-1}$, $k_s = 4\text{W}\cdot\text{m}^{-1}\cdot\text{K}^{-1}$, $k_l = 8\text{W}\cdot\text{m}^{-1}\cdot\text{K}^{-1}$, and $L = 10\text{kJ/kg}$. The thermal simulation is performed until a steady-state heat transfer is achieved for the particulate system. The particle system is then treated as a one-dimensional continuous medium along the vertical (z) direction. The corresponding equivalent thermal properties of the system are obtained.

Figure 4 shows the temperature distribution of Sample 1 ($\nu_s = 0.6$). During the initial heating period, the capsules near the top are heated up while the remaining part keep the initial temperature. As time elapses, the temperature rises gradually in the system.

Figure 3: Temperature distributions and time evolutions of the particulate system with PCM capsules

Figure 4: Determination of the effective latent heat (Sample 1)

Table 1: Effective latent heat of the particulate system

Sample	1	2	3
Packing Density ν_s	0.6	0.65	0.7
Freezing Parameter λ	0.0812	0.0789	0.0761
L_{eff} (kJ/Kg) - Eq.(24)	6.0	6.5	7.0
$L_{\text{eff-fit}}$ (kJ/Kg) - Eq.(34)	6.027	6.404	6.880

The phase change times and positions of all the particles in Sample 1 are depicted in Figure 5, and their relation is curve fitted using Equation (33), from which the freezing constant λ is obtained as 0.0812. Then, by applying Equations (24) and (34), the effective latent heat L_{eff} and the fitted one $L_{\text{eff-fit}}$ can be computed. Both values of L_{eff} and $L_{\text{eff-fit}}$ for all the three samples are listed in Table 1. It can be seen that the fitted values of the effective latent heat L_{eff} match with the actual values of the effective latent heat very well, thus demonstrating the validity of the DTEM method.

6 Further Illustrations

Further simulations are performed to show the effectiveness of the DTEM method in modeling heat transfer in particulate systems involving phase change materials.

6.1 Temperature evolution

Another thermal simulation is conducted using Sample 1 where the granular capsules are considered as sensible material by setting the latent heat L to be 0. Figure 5(a) shows the temperature profile of Sample 1 at different heights for various time instances. A similar profile for the phase change material used in the previous simulations is also displayed in Figure 5(b) for comparison. The top (z=0m) and bottom (z=5m) boundaries of Sample 1 have a constant temperature of 100 ° C and 60 ° C respectively. The initial temperature of all the capsules in the sample is 60 ° C. The heat flux flows from the top to the bottom through the granular capsules. The temperature of the capsules increases during the heat-absorbing process. Heat conduction between two capsules occurs because of their temperature difference.

The phase change material has the ability to absorb large amount of heat without changing its temperature. Thus it takes longer for heat to transfer from the top to the bottom of the phase change materials in the sample. Fig. 5 (a) shows that at the time 600s, the heat transfer process is almost completed in the whole sample for the sensible materials; while Fig. 5(b) indicates that only just over 1/10 of the sample o phase change materials is affected by the heat transfer at the same time. Also, the sample with sensible material reaches the steady-state temperature distribution in about 800s, while for the system with phase change materials, due to the notable heat storage capacity, the same process takes more than 18000s, which is more than 20 times that of the sensible one.

This obvious significance can also be observed from the temperature evolution of the particles at different heights as shown in Figure 6. Capsules at five different heights are selected and their temperatures are depicted against time. For the capsules of sensible material, the temperature increases linearly and reaches to the final temperature very quickly.

Figure 5: Temperature profiles and evolutions of the particulate system with two different materials at different time instances

Figure 6: Temperature evolutions of the particulate system with two different materials at different heights

6.2 Effect of capsule size and packing density

Additional two samples with PCM capsules with different radius ranges but a constant packing density $\nu_s = 0.6$ are generated. The resulting three samples are termed as small (0.04-0.05m), middle (0.05-0.06m) and large (0.06-0.07m). Figure 7(a) show the total melt fraction of the particulate system with different capsule sizes. It can be seen that the samples with smaller capsules taking less time for charging which indicates the same phenomenon as pointed in the previous research [53], but the effect is weak here. This difference is caused by the dissimilarity of the packing configuration of the samples with different particle sizes. The detailed explanation can be found in the work of [54, 55]. Figure 7(b) shows the evolutions of the total melt fraction of the three samples with different packing densities. The difference between these cases is obvious. The sample with the largest packing density attains the complete melting position quickest. The time needed for the loosest sample to reach the final state is more than three times than that of the densest sample. This is because that a denser sample has a larger effective thermal conductivity which can be seen in Table 2 below.

Figure 7: Melt fraction evolutions of the particulate system with different particle sizes and packing densities

6.3 Determination of effective thermal conductivity

As described in Section 4, the effective thermal properties can be calculated from the numerical results. Simulations are conducted on five different samples with different particle size distributions or packing densities as shown in Table 2. In the current simulations, the temperatures are specified at the top and bottom boundaries of the samples, and all the other boundaries are isolated. So only the thermal conductivity along the z direction is determined.

Take Sample 1 as an example. The heat flux at the state of heat equilibrium is obtained when the heat flux at the top and bottom of the sample are equal. Thus, the average heat flux $\langle q'' \rangle = 374.44\,\mathrm{W\,m^{-2}}$ is shown in Figure 8(b). The average temperature gradient is determined by

fitting the temperature distribution using a linear relation which leads to $\langle \nabla T \rangle = 6.92\,\mathrm{K/m}$ as shown in Figure 8(a). Then, by using Equation (22), the effective thermal conductivity is computed as shown in Table 2. The effective thermal conductivity of the other samples are calculated by the same method and listed in Table 2. It can be observed that the effective thermal conductivity is affected significantly by the packing density of a sample while the particle size distribution has a minor effect on the conductivity.

Figure 8: Steady-state particle temperature distribution (a) and heat flux evolutions at the boundaries (b) for Sample 1

Table 2: Effective thermal conductivity of the particulate system

Sample	1	2	3	4	5
Packing density ν_s	0.6	0.65	0.7	0.6	0.6
Radius r /m	0.05-0.06	0.05-0.06	0.05-0.06	0.04-0.05	0.06-0.07
K_{eff} (W/mK)	54.08	137.95	236.66	55.85	48.61

6.4 Effects of thermal induced particle size and packing configuration changes

The size change of particles due to thermal expansion will cause the increase of packing density and the particle rearrangement of the granular system. The consequence of particle rearrangement induced by the thermal excitation may be similar to that caused by difference packing configurations.

Three particle packings are generated using the same parameters as in Sample 2. The only difference between these packings is that they are generated using different random seeds. The same thermal simulations are conducted on these three packings with or without considering the thermal induced size expansion. The particle size expansion is considered following Equation (7). The thermal expansion coefficient is set to be $\beta = 10^{-4}\,\mathrm{K}^{-1}$ based on [56]. The curve fitted finial steady-state temperature distributions and phase change times of these six cases are shown in Figure 10(a) and (b) respectively.

Figure 9: Final temperature distribution (a) and phase change time (b) for different packings with or without size change effect

Comparing the phase change times of the same packing with or without size change in Figure 9(b), it can be seen that the heat transfer is slightly quicker when the size expansion is taken into account in the simulation, as expected. However, the difference is not significant and comparable with the difference caused by different random packing configurations with the same packing density. Therefore, to reduce the computation time and improve the simulation efficiency, it is a reasonable choice to conduct the thermal modelling without considering the size expansion of particles.

7 Conclusion

This work has developed an enthalpy based discrete thermal modelling framework for particulate systems with phase change materials which can consider both the heat conduction process and the phase change transition. The proposed algorithm is numerically very simple and effective. In addition, the equivalent thermal properties of bulk particle materials with phase change have also been derived based on a simple multi-scale modelling scheme. The proposed methodology is assessed by solving a particle version of the classic one-phase Stenfan melting problem. Additional numerical simulations have also been conducted to illustrate the effectiveness of this modelling framework.

The effect of capsule size and packing density can be evaluated directly in the current DTEM method. A particle system of phase change materials with smaller capsules or larger packing densities takes lesser time for charging or discharging. The effective thermal conductivity is affected significantly by the packing density while the particle size distribution has a minor effect. The effect of thermal induced particle size change is not predominant when the temperature involved is low and within a narrow range.

It is noted, however, that the current method can only consider the solid component of the heat storage system without considering heat transfer through fluid phases or by convection. In addition, PCM capsules are treated as spheres with a homogeneous property, thus a possible detailed structure of real PCM capsules is not the focus of the current work.

References

[1] Frédéric Kuznik, Damien David, Kevyn Johannes, and Jean-Jacques Roux. A review on phase change materials integrated in building walls. *Renewable and Sustainable Energy Reviews*, 15(1):379–391, 2011.

[2] MK Anuar Sharif, AA Al-Abidi, Sohif Mat, Kamaruzzaman Sopian, Mohd Hafidz Ruslan, MY Sulaiman, and MAM Rosli. Review of the application of phase change material for heating and domestic hot water systems. *Renewable and Sustainable Energy Reviews*, 42:557–568, 2015.

[3] Xiwen Cheng, Xiaoqiang Zhai, and Ruzhu Wang. Thermal performance analysis of a packed bed cold storage unit using composite pcm capsules for high temperature solar cooling application. *Applied thermal engineering*, 100:247–255, 2016.

[4] Hao Peng, Rui Li, Xiang Ling, and Huihua Dong. Modeling on heat storage performance of compressed air in a packed bed system. *Applied energy*, 160:1–9, 2015.

[5] María Asunción Izquierdo Barrientos. Heat transfer and thermal storage in fixed and fluidized beds of phase change materials. 2014.

[6] T Saitoh and K Hirose. High-performance phase-change thermal energy storage using spherical capsules. *Chemical Engineering Communications*, 41(1-6):39–58, 1986.

[7] Keumnam Cho and SH Choi. Thermal characteristics of paraffin in a spherical capsule during freezing and melting processes. *International journal of heat and mass transfer*, 43(17):3183–3196, 2000.

[8] Eduard Oró, Albert Castell, Justin Chiu, Viktoria Martin, and Luisa F Cabeza. Stratification analysis in packed bed thermal energy storage systems. *Applied energy*, 109:476–487, 2013.

[9] D Vortmeyer and RJ Schaefer. Equivalence of one-and two-phase models for heat transfer processes in packed beds: one dimensional theory. *Chemical Engineering Science*, 29(2):485–491, 1974.

[10] To EW Schumann. Heat transfer: a liquid flowing through a porous prism. *Journal of the Franklin Institute*, 208(3):405–416, 1929.

[11] Alvaro de Gracia and Luisa F Cabeza. Numerical simulation of a pcm packed bed system: a review. *Renewable and Sustainable Energy Reviews*, 69:1055–1063, 2017.

[12] Ciril Arkar and Sašo Medved. Influence of accuracy of thermal property data of a phase

change material on the result of a numerical model of a packed bed latent heat storage with spheres. *Thermochimica Acta*, 438(1-2):192–201, 2005.

[13] KAR Ismail and JR Henriquez. Numerical and experimental study of spherical capsules packed bed latent heat storage system. *Applied Thermal Engineering*, 22(15):1705–1716, 2002.

[14] Yvan Dutil, Daniel R Rousse, Nizar Ben Salah, Stéphane Lassue, and Laurent Zalewski. A review on phase-change materials: mathematical modeling and simulations. *Renewable and sustainable Energy reviews*, 15(1):112–130, 2011.

[15] Peter A Cundall and Otto DL Strack. A discrete numerical model for granular assemblies. *geotechnique*, 29(1):47–65, 1979.

[16] ML Hunt. Discrete element simulations for granular material flows: effective thermal conductivity and self-diffusivity. *International journal of heat and mass transfer*, 40(13):3059–3068, 1997.

[17] Watson L Vargas and JJ McCarthy. Heat conduction in granular materials. *AIChE Journal*, 47(5):1052–1059, 2001.

[18] Watson L Vargas and JJ McCarthy. Stress effects on the conductivity of particulate beds. *Chemical Engineering Science*, 57(15):3119–3131, 2002.

[19] Bodhisattwa Chaudhuri, Fernando J Muzzio, and M Silvina Tomassone. Modeling of heat transfer in granular flow in rotating vessels. *Chemical Engineering Science*, 61(19):6348–6360, 2006.

[20] YT Feng, K Han, CF Li, and DRJ Owen. Discrete thermal element modelling of heat conduction in particle systems: Basic formulations. *Journal of Computational Physics*, 227(10):5072–5089, 2008.

[21] YT Feng, K Han, and DRJ Owen. Discrete thermal element modelling of heat conduction in particle systems: pipe-network model and transient analysis. *Powder Technology*, 193(3):248–256, 2009.

[22] John C Steuben, Athanasios P Iliopoulos, and John G Michopoulos. Discrete element modeling of particle-based additive manufacturing processes. *Computer Methods in Applied Mechanics and Engineering*, 305:537–561, 2016.

[23] S Haeri, Y Wang, O Ghita, and J Sun. Discrete element simulation and experimental study of powder spreading process in additive manufacturing. *Powder Technology*, 306:45–54,

2017.

[24] HW Zhang, Q Zhou, HL Xing, and H Muhlhaus. A dem study on the effective thermal conductivity of granular assemblies. *Powder technology*, 205(1-3):172–183, 2011.

[25] Yuanbo Liang, Haiying Niu, and Yafei Lou. Expression for etc of the solid phase of randomly packed granular materials. *Applied Thermal Engineering*, 109:44–52, 2016.

[26] Akhil Reddy Peeketi, Marigrazia Moscardini, Akhil Vijayan, Yixiang Gan, Marc Kamlah, and Ratna Kumar Annabattula. Effective thermal conductivity of a compacted pebble bed in a stagnant gaseous environment: An analytical approach together with dem. *Fusion Engineering and Design*, 130:80–88, 2018.

[27] J Stefan. Uber einige probleme der theorie der warmeletung. *Sitzer. Wien. Akad. Math. Naturw.*, 98:473–484, 1889.

[28] Yanio E Milian, Andrea Gutierrez, Mario Grageda, and Svetlana Ushak. A review on encapsulation techniques for inorganic phase change materials and the influence on their thermophysical properties. *Renewable and Sustainable Energy Reviews*, 73:983–999, 2017.

[29] A Jamekhorshid, SM Sadrameli, and Mohammed Farid. A review of microencapsulation methods of phase change materials (pcms) as a thermal energy storage (tes) medium. *Renewable and Sustainable Energy Reviews*, 31:531–542, 2014.

[30] Mohamed Rady. Granular phase change materials for thermal energy storage: experiments and numerical simulations. *Applied Thermal Engineering*, 29(14-15):3149–3159, 2009.

[31] L Xia, P Zhang, and RZ Wang. Numerical heat transfer analysis of the packed bed latent heat storage system based on an effective packed bed model. *Energy*, 35(5):2022–2032, 2010.

[32] KAR Ismail and R Stuginsky Jr. A parametric study on possible fixed bed models for pcm and sensible heat storage. *Applied Thermal Engineering*, 19(7):757–788, 1999.

[33] Selvan Bellan, Tanvir E Alam, José González-Aguilar, Manuel Romero, Muhammad M Rahman, D Yogi Goswami, and Elias K Stefanakos. Numerical and experimental studies on heat transfer characteristics of thermal energy storage system packed with molten salt pcm capsules. *Applied thermal engineering*, 90:970–979, 2015.

[34] JGH Borkink and KR Westerterp. Influence of tube and particle diameter on heat transport in packed beds. *AIChE journal*, 38(5):703–715, 1992.

[35] George Keith Batchelor and RW O'brien. Thermal or electrical conduction through a granular material. *Proc. R. Soc. Lond. A*, 355(1682):313–333, 1977.

[36] Watson L Vargas and Joseph J McCarthy. Thermal expansion effects and heat conduction in granular materials. *Physical Review E*, 76(4):041301, 2007.

[37] Xiao-Liang Wang and Dong-Yun Bai. Thermal expansion and thermal fluctuation effects in a binary granular mixture. *International Journal of Heat and Mass Transfer*, 116:84–92, 2018.

[38] Xiao-Liang Wang and Dong-Yun Bai. Thermal cycling leads grains to more homogeneous force networks and energy repartition. *Powder technology*, 339:111–118, 2018.

[39] M Michael Yovanovich. Four decades of research on thermal contact, gap, and joint resistance in microelectronics. *IEEE transactions on components and packaging technologies*, 28(2):182–206, 2005.

[40] MG Cooper, BB Mikic, and MM Yovanovich. Thermal contact conductance. *International Journal of heat and mass transfer*, 12(3):279–300, 1969.

[41] BB Mikić. Thermal contact conductance; theoretical considerations. *International Journal of Heat and Mass Transfer*, 17(2):205–214, 1974.

[42] Yuanbo Liang and Xikui Li. A new model for heat transfer through the contact network of randomly packed granular material. *Applied Thermal Engineering*, 73(1):984–992, 2014.

[43] PFC3D Itasca. Particle flow code in 3 dimensions, user's guide, 2008.

[44] Shazim Ali Memon. Phase change materials integrated in building walls: A state of the art review. *Renewable and sustainable energy reviews*, 31:870–906, 2014.

[45] S Tavman and IH Tavman. Measurement of effective thermal conductivity of wheat as a function of moisture content. *International communications in heat and mass transfer*, 25(5):733–741, 1998.

[46] Zhou Zhao, KM Feng, and YJ Feng. Theoretical calculation and analysis modeling for the effective thermal conductivity of li4sio4 pebble bed. *Fusion Engineering and Design*, 85(10-12):1975–1980, 2010.

[47] Katalin Bagi. Stress and strain in granular assemblies. *Mechanics of materials*, 22(3):165–177, 1996.

[48] W Ehlers, E Ramm, S Diebels, and GA dAddetta. From particle ensembles to cosserat continua: homogenization of contact forces towards stresses and couple stresses.

International Journal of Solids and Structures, 40(24):6681–6702, 2003.

[49] Ching S Chang and Matthew R Kuhn. On virtual work and stress in granular media. *International Journal of Solids and Structures*, 42(13):3773–3793, 2005.

[50] XH Wen, LJ Durlofsky, and MG Edwards. Use of border regions for improved permeability upscaling. *Mathematical Geology*, 35(5):521–547, 2003.

[51] Marek Błasik. Numerical scheme for the one-phase 1d stefan problem using curvilinear coordinates. *Scientific Research of the Institute of Mathematics and Computer Science*, 11(3):9–14, 2012.

[52] HS Carslaw and JC Jaeger. *Conduction of heat in solids: Oxford Science Publications*. Oxford, England, 1959.

[53] A Felix Regin, SC Solanki, and JS Saini. An analysis of a packed bed latent heat thermal energy storage system using pcm capsules: Numerical investigation. *Renewable energy*, 34(7):1765–1773, 2009.

[54] YT Feng, Kuanjin Han, DRJ Owen, and J Loughran. On upscaling of discrete element models: similarity principles. *Engineering Computations*, 26(6):599–609, 2009.

[55] YT Feng and DRJ Owen. Discrete element modelling of large scale particle systemsi: exact scaling laws. *Computational Particle Mechanics*, 1(2):159–168, 2014.

[56] RG Craig, JD Eick, and FA Peyton. Properties of natural waxes used in dentistry. *Journal of Dental Research*, 44(6):1308–1316, 1965.

Graphical abstract

Highlights

- Investigated the particulate system of PCM from the discontinuous point of view
- Developed an enthalpy based discrete thermal modelling (DTEM) framework
- Validated the algorithm by solving the classic Stefan melting problem
- Derived the equivalent thermal properties based on a multi-scale modelling scheme

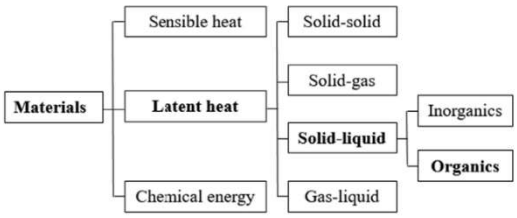

(a) Classification of energy storage materials

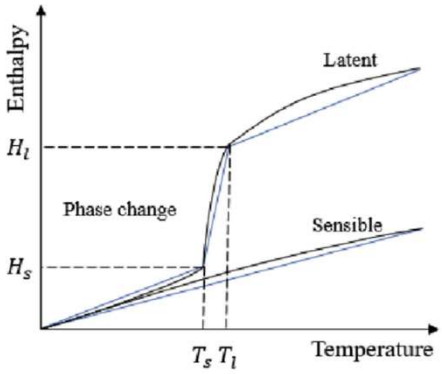

(b) Enthalpy variation with temperature

Figure 1

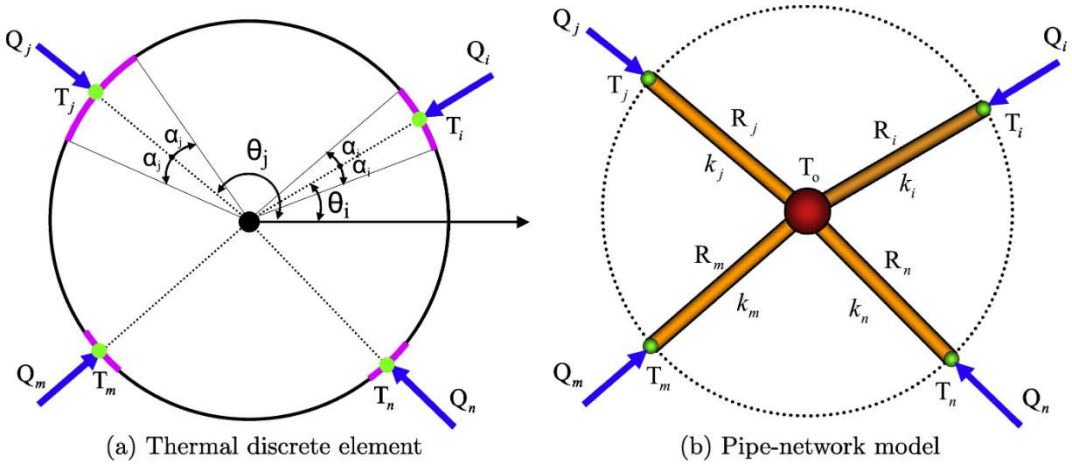
Q_j
Q_i
T_j
T_i
α_j
α_j
θ_j
α_i
α_i
θ_i
Q_m
T_m
T_n
Q_n
(a) Thermal discrete element
Q_j
Q_i
T_j
R_j
R_i
T_i
k_j
T_o
k_i
R_m
R_n
k_m
k_n
Q_m
T_m
T_n
Q_n
(b) Pipe-network model

Figure 2

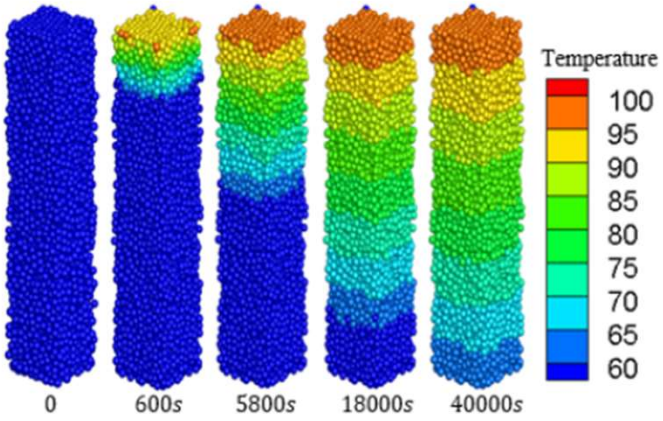
Temperature
100
95
90
85
80
75
70
65
60
0
600s
5800s
18000s
40000s

Figure 3

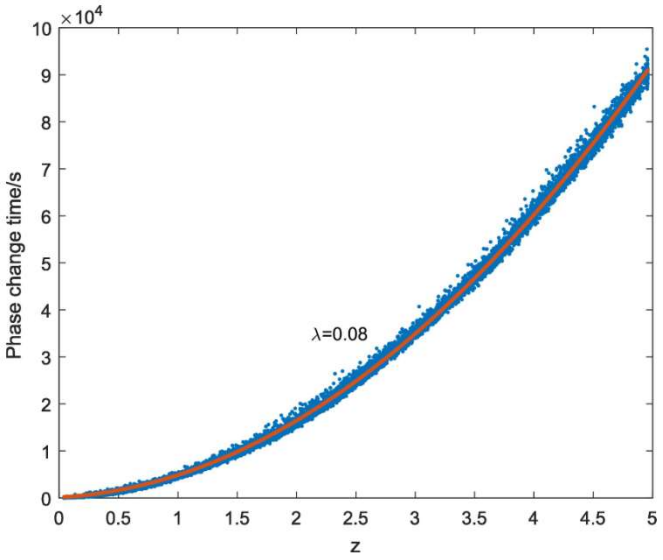
×10^4
10
9
8
7
6
5
4
3
2
1
0
Phase change time/s
λ=0.08
0
0.5
1
1.5
2
2.5
3
3.5
4
4.5
5
z

Figure 4

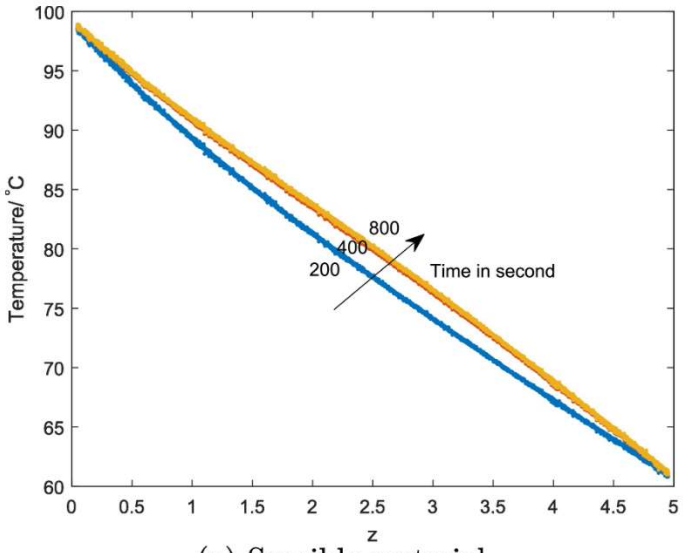

(a) Sensible material

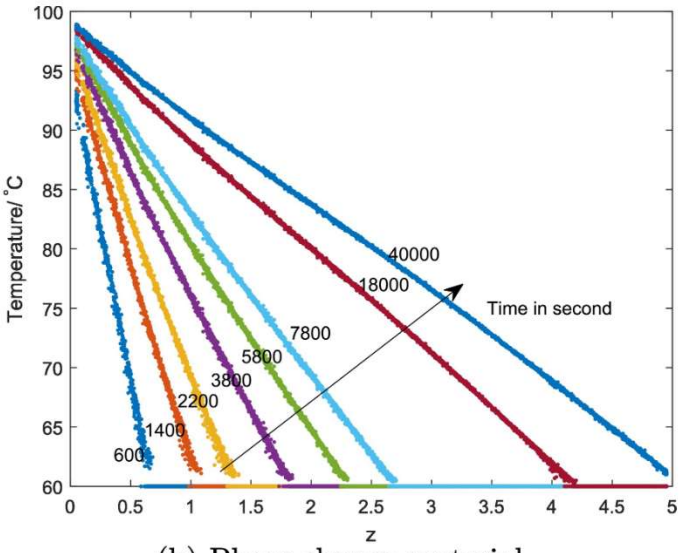

(b) Phase change material

Figure 5

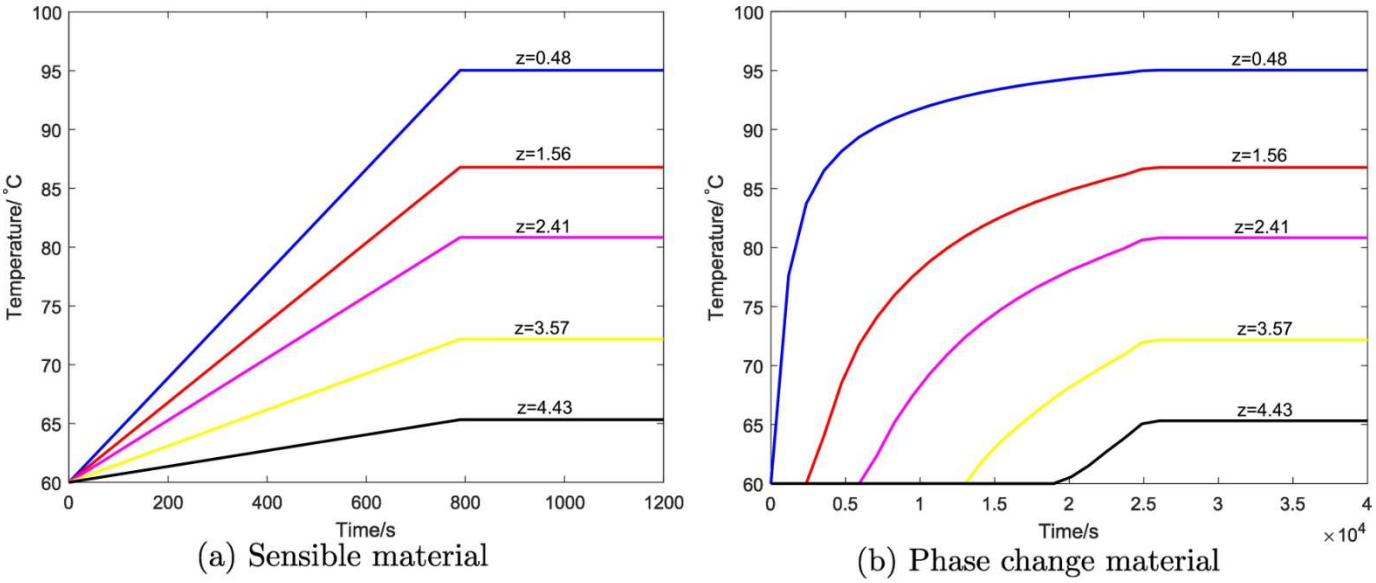

(a) Sensible material (b) Phase change material

Figure 6

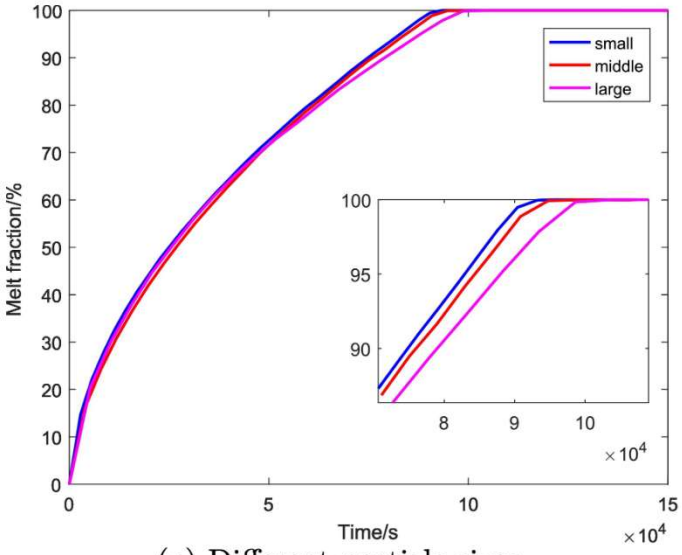

(a) Different particle sizes

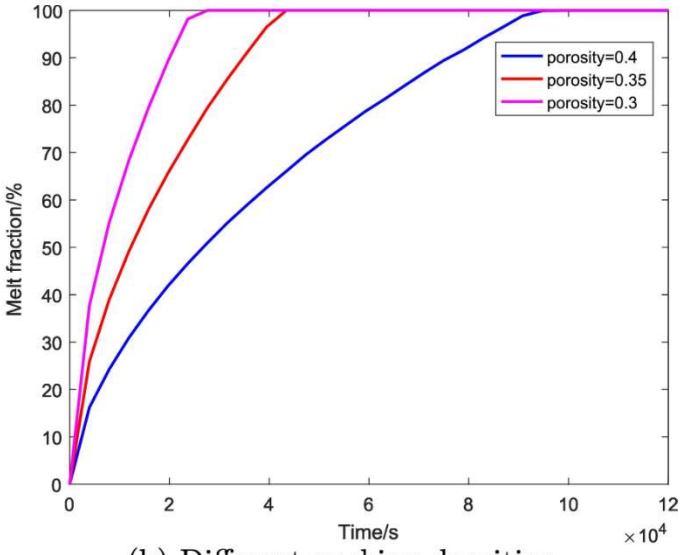

(b) Different packing densities

Figure 7

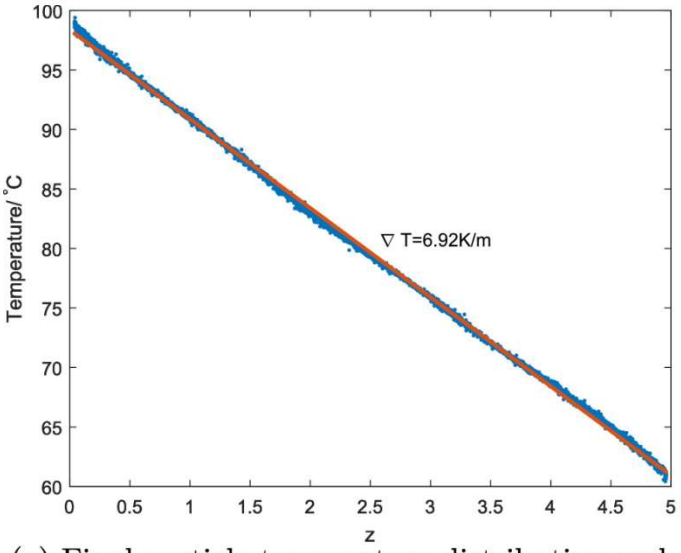

(a) Final particle temperature distribution and fitted linear temperature distribution with computed gradient

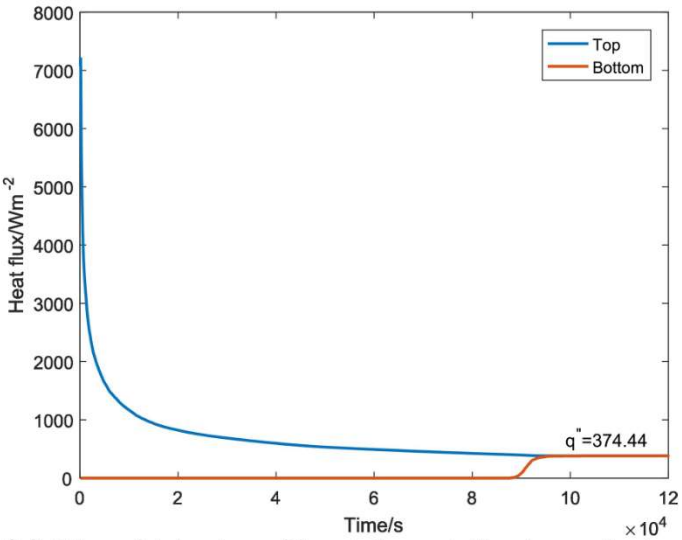

(b) Time histories of heat flux at the boundaries

Figure 8

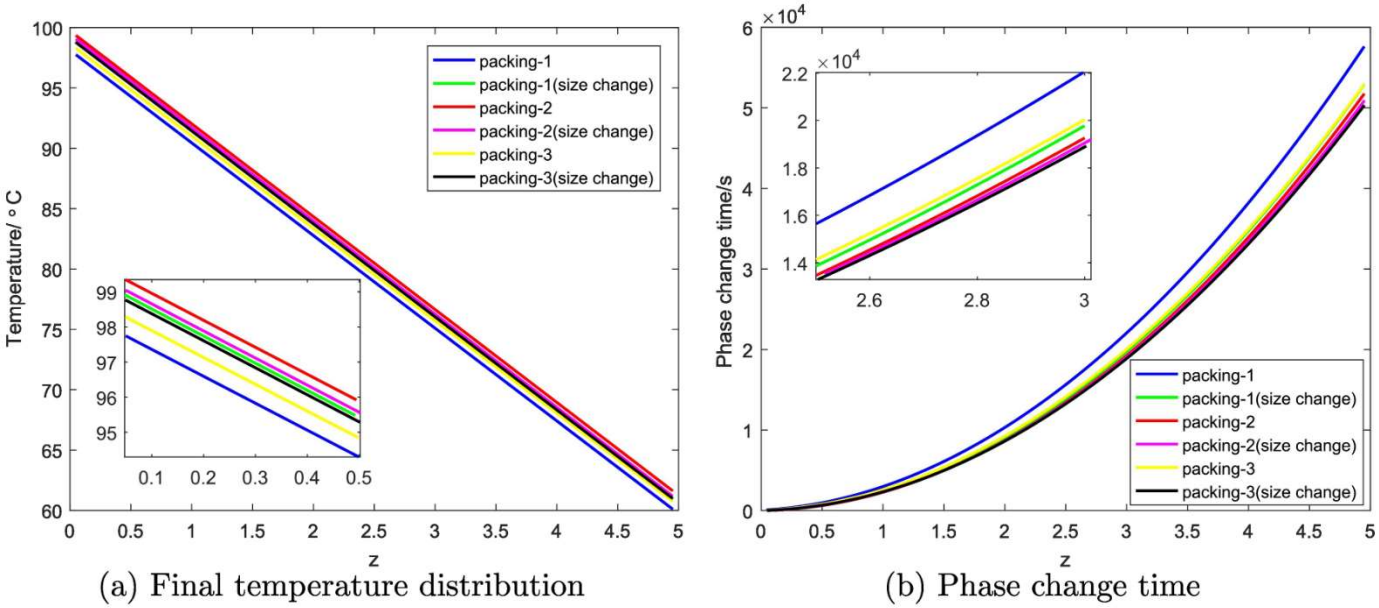

(a) Final temperature distribution

(b) Phase change time

Figure 9